 ©2015 Kvantovaya Elektronika and Turpion Ltd

PACS numbers: 42.65.An; 42.65.Re; 42.60.Jf
DOI: 10.1070/QE2015v045n05ABEH015763

# Enhancement of temporal contrast of high-power laser pulses in an anisotropic medium with cubic nonlinearity

M.S. Kuz'mina, E.A. Khazanov

***Abstract.*** **We consider the methods for enhancing the temporal contrast of super-high-power laser pulses, based on the conversion of radiation polarisation in a medium with cubic nonlinearity. For a medium with weak birefringence and isotropic nonlinearity, we propose a new scheme to enhance the temporal contrast. For a medium with anisotropic nonlinearity, the efficiency of the temporal contrast optimisation is shown to depend not only on the spatial orientation of the crystal and *B*-integral, but also on the type of the crystal lattice symmetry.**

***Keywords:*** *temporal contrast, femtosecond laser pulses, anisotropic medium with cubic nonlinearity, B-integral.*

## 1. Introduction

The development of chirped pulse amplification (CPA) technology has led to the fabrication of petawatt lasers. Petawatt lasers offer great opportunities for fundamental study of the interaction of laser radiation with matter in the ultra-relativistic regime. A femtosecond laser pulse generally has a complex temporal structure. The main pulse is preceded by pre-pulses of lower intensity, resulting from different processes occurring in the laser system, and the main pulse has a wide picosecond pedestal. Because pre-pulses can simply destroy the target structure or distort the results of studies of the interaction of laser pulses with matter before the arrival of the main pulse, it is necessary to minimise the intensity of pre-pulses, in other words – to enhance the femtosecond pulse contrast.

If no special methods are used, the temporal contrast of a pulse at the compressor output will be several orders of magnitude less than that required (at least $10^{10}$) for many applications. The temporal contrast can be enhanced using plasma mirrors [1, 2] and devices based on second harmonic generation [3, 4]. The energy loss in this case is 30%–50% with the plasma mirror being replaced after each 'shot', whereas the second harmonic generation requires thin, large-aperture nonlinear crystals, the production of which causes considerable practical difficulties.

The double chirp pulse amplification (DCPA) technique has become widespread, when, after a system of preliminary laser amplification, the contrast is enhanced at milli-joule energy [5]. Temporal and spatial inhomogeneity of laser radiation leads to low efficiency of generation of high-contrast radiation, and therefore use is made of re-stretching and amplification of a femtosecond laser pulse. For this reason, the DCPA technique is not so sensitive to the energy loss, despite the need to install an additional stretcher and a compressor. This allows the use of a nonlinear circular Sagnac interferometer [6], a saturable absorber [7, 8] and devices based on the effects emerging in a medium with cubic nonlinearity: rotation of the polarisation ellipse [9, 10] and generation of orthogonally polarised waves [11, 12], i.e., XPW (cross polarised wave generation). The XPW method is the most promising in terms of enhancing the temporal contrast – a possible increase in contrast is 4–5 orders and is limited by the contrast of polarisers. An additional advantage consists in the ability to simultaneously broaden the spectrum, which can significantly reduce the laser pulse duration. One of the most recent results [13] has been obtained in a scheme with two barium fluoride crystals – linearly polarised light with an intensity of 0.6–0.9 TW cm$^{-2}$ and a Gaussian spatiotemporal profile was converted into orthogonally polarised radiation with an efficiency of 24%–30%. The pulse duration was reduced from 25 to 10 fs, the temporal contrast was enhanced by at least two orders of magnitude and amounted to $10^{10}$. A further increase (estimated at up to 40%) in the generation efficiency of orthogonally polarised radiation is associated with an increase in the input radiation intensity, which is limited by a threshold of small-scale self-focusing development.

Despite considerable progress in the development of the XPW method, there are new works where use is made of cubic nonlinearity of a medium. For example, Liu et al. [14] use self-diffraction. When two intersecting laser beams interact, an interference light field is formed, under whose action in a medium there occurs a periodic variation in the dielectric constant and, as a consequence, there appear beams propagating in new directions. The advantage of this method, as compared with XPW, consists in the absence of limitation on the enhancement of the temporal contrast due to the contrast of the polariser; however, the conversion efficiency is low and amounts to 12%.

In Section 2 we describe the traditional method of contrast enhancement, based on the rotation of the polarisation ellipse in an isotropic nonlinear medium. In Section 3 we propose a new method utilising the effect of the polarisation-ellipse rotation in a birefringent medium. This method is compared with the traditional one.

The authors of [11, 13] present the results of the experiments to enhance the temporal contrast in the process of generation of orthogonally polarised radiation in two (barium fluoride and calcium fluoride) nonlinear crystals. However,

**M.S. Kuz'mina, E.A. Khazanov** Institute of Applied Physics, Russian Academy of Sciences, ul. Ul'yanova 46, 603950 Nizhny Novgorod, Russia; e-mail: kmsnn@mail.ru, khazanov@appl.sci-nnov.ru

Received 29 January 2015; revision received 10 February 2015
Kvantovaya Elektronika **45** (5) 426–433 (2015)
Translated by I.A. Ulitkin

from the viewpoint of improving the effectiveness of this method, other nonlinear media, including uniaxial crystals, may be of interest. In the literature, the problem of an anisotropic crystal and the criteria for finding an optimal nonlinear crystal and its optimal orientation are underrepresented. In Section 4 we consider the possibility of using nonlinear crystals (cubic and uniaxial) with different types of the crystal lattice symmetry for XPW and summarise the known literature data on cubic nonlinearity tensors of different crystals. Note that the calculation results presented in this paper are obtained in the plane wave approximation.

## 2. Isotropic medium

Before considering anisotropic media, we present the main results of studies aimed at enhancing the contrast of an isotropic medium. The method of the temporal contrast enhancement, based on the effect of the polarisation-ellipse rotation in an isotropic medium with cubic nonlinearity, is investigated in detail in [9, 10]. The scheme of this method is shown in Fig. 1. Nonlinear element (NE) (*3*) is placed between crossed polarisers (*1*) and two quarter-wave plates (*2*), whose optical axes are rotated around the $z$ axis by the angles $\theta$ and $\theta + \pi/2$, respectively. Varying $\theta$ one can obtain any polarisation ellipticity at the NE input. At a low intensity, the linearly polarised light preserves the type of polarisation after the second quarter-wave plate and passes completely through the second crossed polariser. With increasing intensity, the polarisation of light after the second quarter-wave plate becomes elliptical due to the rotation of the polarisation ellipse in the NE. In this case, only part of the laser light passes through the second crossed polariser: the radiation component with a polarisation orthogonal to the initial one is coupled out from the system by the polariser. This scheme of the temporal contrast enhancement allows one to separate low-intensity (pre-pulse) radiation from high-intensity (main pulse) radiation.

The equations for the clockwise and counterclockwise circularly polarised components of the light field $E_\pm = (E_x \pm iE_y)/\sqrt{2}$ have the form [15, 16]

$$\frac{dE_+}{dz} = \frac{i\pi k_0 \chi_{xxxx}}{n_0}(|E_+|^2 + 2|E_-|^2)E_+,$$
$$\frac{dE_-}{dz} = \frac{i\pi k_0 \chi_{xxxx}}{n_0}(|E_-|^2 + 2|E_+|^2)E_-, \quad (1)$$

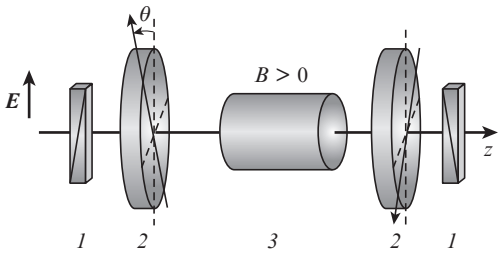


**Figure 1.** Scheme of the method for enhancing the temporal contrast, based on the effect of the polarisation-ellipse rotation in an isotropic medium with cubic nonlinearity: (*1*) crossed polarisers; (*2*) π/4 plates; (*3*) NE.

where $E_x$ and $E_y$ are the transverse Cartesian components of the electric field vector $\boldsymbol{E}$; $\chi_{xxxx}$ is the diagonal component of a fourth-rank nonlinear susceptibility tensor $\chi^{(3)}$; $k_0 = 2\pi/\lambda$; $\lambda$ is the wavelength; and $n_0$ is the linear part of the refractive index of a medium. Here we have only taken into account the electronic mechanism of nonlinearity, caused by the electronic polarisability of atoms and molecules of the medium [17]. The solution to (1) has the form

$$E_\pm = E_{0\pm}\exp\{iB\{1 \pm {}^1/_3\cos[(\pi/2)(\Sigma + 1)]\}\},$$

where the value $\Sigma = (4/\pi)\arctan(|E_-|/|E_+|) - 1$ defines the polarisation ellipticity; $B$-integral is given by the expression

$$B = \frac{12\pi^2 k_0}{n_0^2 c}\chi_{xxxx} IL; \quad (2)$$

$c$ is the velocity of light in vacuum; $I$ is the intensity of light; and $L$ is the NE length. The angle of the polarisation-ellipse rotation at the nonlinear medium output is $\Phi_{NL} = (B/3)\times\cos[(\pi/2)(\Sigma + 1)]$, and its dependence on $B$ and $\Sigma$ is shown in Fig. 2a.

An important characteristic of the process of the temporal contrast enhancement is the efficiency $\eta$, which is defined as the proportion of the intensity of the radiation component with a polarisation that is orthogonal to that which would have been in the absence of nonlinearity. Knowing the angle of rotation, $\Phi_{NL}$, for the dependence $\eta(B, \Sigma)$ one can easily obtain an analytical expression

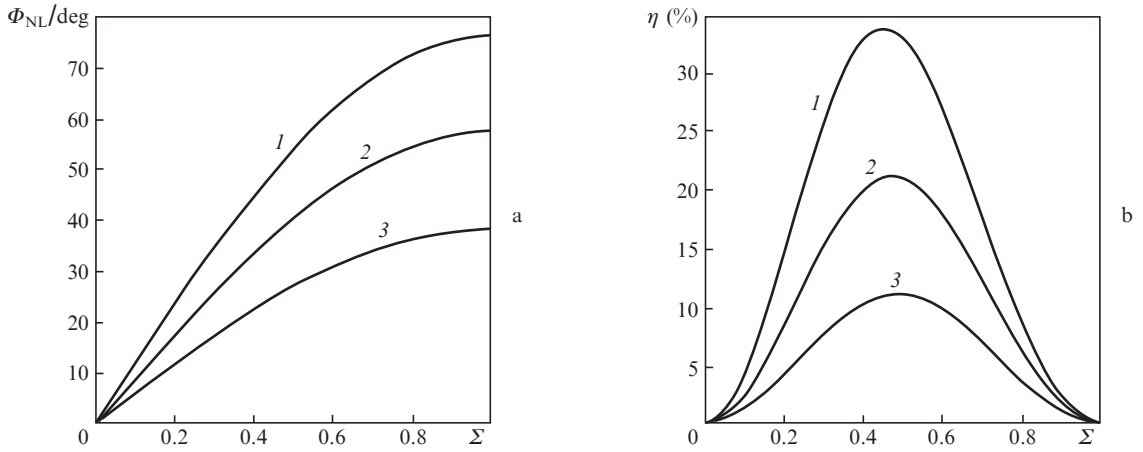


**Figure 2.** Dependences of (a) the angle of the polarisation-ellipse rotation and (b) conversion efficiency $\eta$ on ellipticity $\Sigma$ at $B =$ (*1*) 4, (*2*) 3 and (*3*) 2.

$$\eta = \cos^2\left(\frac{\pi}{2}\Sigma\right)\sin^2\left[\frac{B}{3}\sin\left(\frac{\pi}{2}\Sigma\right)\right].$$

One can see from Fig. 2b that the optimal (in terms of the conversion efficiency of the polarisation) polarisation ellipticity $\Sigma$ varies slightly with increasing $B$-integral and is approximately equal to ±0.5 [+ (–) refers to the clockwise polarised (counter-clockwise polarised) wave]. In this case, the angle $\theta = 22.5°$. This conclusion can be explained by referring to Fig. 2a. The angle of the polarisation-ellipse rotation $\Phi_{NL} = 0$ in the case of propagation of linearly polarised light ($\Sigma = 0$) in a medium for any values of $B$. When light is circularly polarised ($\Sigma = \pm 1$), the angle of rotation is maximal. However, the highest conversion efficiency occurs at the intermediate ellipticity $\Sigma \approx \pm 0.5$, because at $\Sigma$, close to ±1, the polarisation is close to circular, and its rotation even by 90° only slightly changes the polarisation.

## 3. Weakly birefringent and nonlinear isotropic medium

In [18], we investigated the method of polarisation distortion suppression in active elements of laser amplifiers, caused by the appearance of thermally induced birefringence and by the effect of cubic nonlinearity. Using the plane-wave approximation we observed significant residual thermally induced depolarisation at $B > 0$ in a scheme consisting of two identical active elements and a 90-degree polarisation rotator. The dependence of the degree of depolarisation of initially linearly polarised radiation on the thermally induced phase difference $\delta$ of the eigenwaves of a medium was found to be nonmonotonic. The maximum of the polarisation degree was achieved at a small thermally induced birefringence – $\delta = 3\pi/5$, which corresponds to weak anisotropy of a medium. It was assumed that the distortion of the nonlinear susceptibility tensor of a initially isotropic medium due to thermal stresses is a second-order effect, i.e., nonlinear properties of the medium remain isotropic.

In this paper, we investigate the possibility of using this effect for enhancing the temporal contrast of high-power laser pulses. Let us consider two NEs with the optical axes rotated through 90° relative to each other (Fig. 3). The NEs are made of a material having weak and uniform birefringence in the cross section. An example of a medium with such properties is a plate of a crystal with symmetry groups 622, 6mm, $\bar{6}$m2, 6/mmm, 32, 3m and $\bar{3}$m, in which the optical axis is tilted at a small angle to the axis of laser radiation propagation (see Section 4). Another example would be a plastic plate, a weak birefringence in which occurs due to a uniform mechanical deformation. Full details of this example can be found in the theoretical and experimental studies [19, 20]. Note that due to a virtually unlimited aperture, plastic can be used not only in the DCPA technique, but also directly at the output of petawatt lasers.

We investigate the conversion of laser light polarisation upon passage through the scheme shown in Fig. 3. Let the initial polarisation be linear and the electric field strength vector make an angle $\varphi$ with the $x$ axis. Propagation of laser radiation in an isotropic medium with cubic nonlinearity and anisotropic refractive index is described by the system of differential equations [21]:

$$\frac{dE_x}{dz} = \frac{3i\pi k_0}{2n_x}\chi_{xxxx}[|E_x|^2E_x + {}^1\!/_3(2|E_y|^2E_x + E_y^2E_x^*)] - \frac{ik_0}{2}(n_x - n_y)E_x,$$

$$\frac{dE_y}{dz} = \frac{3i\pi k_0}{2n_y}\chi_{xxxx}[|E_y|^2E_y + {}^1\!/_3(2|E_x|^2E_y + E_x^2E_y^*)] + \frac{ik_0}{2}(n_x - n_y)E_y, \quad (3)$$

where $n_x$ and $n_y$ are the refractive indices for orthogonally polarised eigenwaves of the medium; and $\delta = k_0(n_x - n_y)L$ is the phase difference of eigenwaves of the medium. It is easy to show that for an isotropic medium, i.e., when $\delta = 0$, system (3), by replacing the variables $E_\pm \to (E_x \pm iE_y)/\sqrt{2}$, transforms to system (1). Equations (3) were solved numerically.

We analyse the influence of $\delta$, $\varphi$ and $B$-integral on the conversion efficiency of linearly polarised light into orthogonally polarised light in the scheme in Fig. 3. From a practical point of view it is convenient that when $B = 0$, the output radiation is linearly polarised. To do this, the phase differences $\delta$ must be equal in magnitude and opposite in sign in two NEs. Let the values of the $B$-integrals of the first and second NEs, $B_1$ and $B_2$, be related by the expression $B_1 = qB_2$, where $q$ takes values from the interval [0; 1], and $B = B_1 + B_2$ is the total $B$-integral.

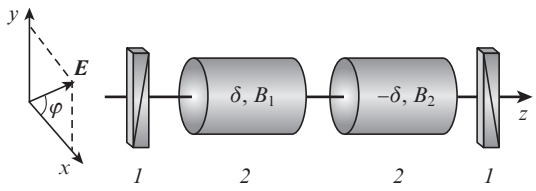


**Figure 3.** Scheme of the method for enhancing the temporal contrast, based on the effect of the polarisation-ellipse rotation in a weakly anisotropic medium with cubic nonlinearity: (*1*) crossed polarisers; (*2*) NE.

In practice, the values of $\delta$ and $\varphi$ are easily varied by selecting the optimal values; therefore, we define the maxima of the function $\eta(\delta,\varphi)$ for different values of $B$ and $B_1$. Each point of the dependences in Fig. 4a is plotted for optimal (the highest $\eta$) values of $\delta_{max}$ and $\varphi_{max}$. It is easy to notice that the maximum of the function $\eta(\delta_{max},\varphi_{max},B_1)$ is achieved at $B_1 = 0$. The obtained result can be explained, if one analyses the dependence of $\eta$ and ellipticity $\Sigma$ of light polarisation at the input to the second NE on the angle $\varphi$ and phase difference $\delta$ (Figs 4b and 4d) at $B_1 = 0$, $B = 3$. When $\delta = \delta_{max}$, $\varphi = \varphi_{max}$, the quantity $\eta$ reaches a maximum, and the ellipticity of polarisation at the input to the second NE is –0.5, which coincides with the optimum value of ellipticity in the scheme with an isotropic medium (Fig. 1). In other words, the first element in this case is simply a phase plate providing the desired ellipticity of polarisation at the input to the second NE. The dependence of the optimal angle $\varphi_{max}$ on $B_1$ at $B = 2, 3, 4$ is shown in Fig. 4c. The optimum value of $\delta$ is weakly dependent on the values of $B$ and $B_1$ and is approximately equal to $0.45\pi$.

For the scheme in Fig. 3 we also investigated the case of propagation of elliptically polarised light. It was found that the value of $\eta$ in this case is less than that for linearly polarised radiation. The results of calculations allow one to abandon the use of less convenient (in terms of the practical application) elliptical polarisation.

Note that at small values of the $B$-integral, the conversion efficiencies of radiation into orthogonally polarised light in the proposed scheme and the scheme in Fig. 1 are comparable,

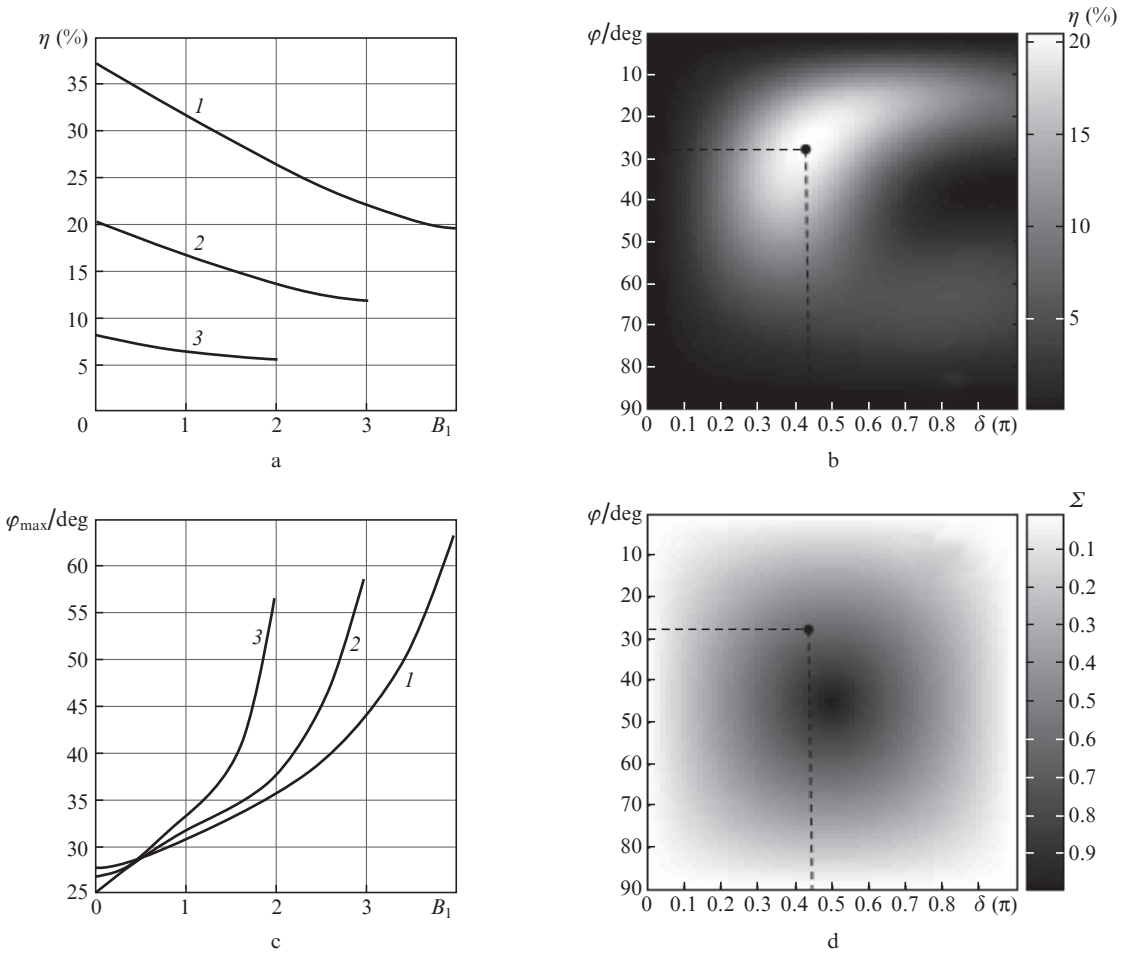


**Figure 4.** Dependences of (a) the conversion efficiency and (c) optimal angle $\varphi_{max}$ at the output of the system in Fig. 3 on the value of the $B$-integral in the first element $B_1$ at $B = (1)$ 4, (2) 3 and (3) 2, as well as dependences of (b) the conversion efficiency and (d) polarisation ellipticity after the first NE on $\delta$ and $\varphi$ at $B = 3$, $B_1 = 0$. Points in Figs 4b and 4d correspond to the optimum values of $\delta$ and $\varphi$.

and at its large values the new scheme exhibits an increase in $\eta$: if $B = 4$, the value of $\eta$ is greater by 5%. Furthermore, the proposed scheme does not require the use quarter-wave plates, which is especially important in the case of large beam apertures.

## 4. Nonlinear anisotropic medium

For an anisotropic medium with cubic nonlinearity, the nonlinear susceptibility tensor has diagonal and off-diagonal components [22]. In this paper we confine ourselves to consideration of a practically convenient case of linear polarisation of the input light and one NE made of an isotropic (cubic) crystal or a uniaxial crystal oriented along the optical axis (Fig. 5). If the uniaxial crystal has another orientation, the significant difference of group velocities of ordinary and extraordinary waves will lead to spatial separation of the input pulse into two pulses. Thus, in the case of the uniaxial crystal, the system of coordinates coincides with the crystal axes. In this case, the form of a system of differential equations for the components of the electric field vectors $E_x$ and $E_y$ depends on the symmetry of the crystal lattice. In general, the system has the form of expressions (4), and in particular cases it is reduced to systems (5) or (6) (the correspondence of systems of equation to symmetry groups is given in Table 1):

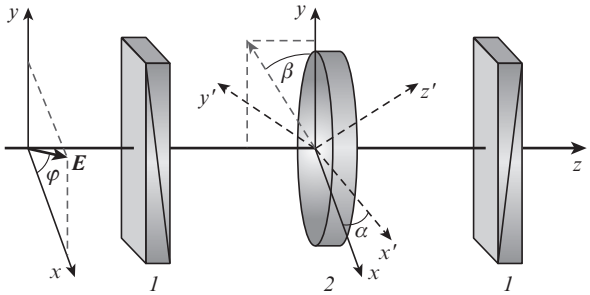


**Figure 5.** Scheme of the method for enhancing the temporal contrast of laser radiation, based on the generation of orthogonally polarised components of radiation in an anisotropic nonlinear medium: (1) crossed polarisers; (2) NE.

$$\frac{dE_x}{dz} = \frac{3i\pi k_0}{2n_o}[\chi_{xxxx}|E_x|^2E_x + \chi_{xxyy}(2|E_y|^2E_x + E_y^2E_x^*) + \chi_{xxxy}(E_x^2E_y^* + 2|E_x|^2E_y - |E_y|^2E_y)],$$

$$\frac{dE_y}{dz} = \frac{3i\pi k_0}{2n_o}[\chi_{xxxx}|E_y|^2E_y + \chi_{xxyy}(2|E_x|^2E_y + E_x^2E_y^*) - \chi_{xxxy}(E_y^2E_x^* + 2|E_y|^2E_x - |E_x|^2E_x)], \quad (4)$$

**Table 1.** Generation efficiency of orthogonally polarised components in uniaxial and cubic crystals.

| Crystal lattice | Symmetry group | Orientation | $\sigma_1$ | $\sigma_2$ | System of equations | $\eta$ |
|---|---|---|---|---|---|---|
| Trigonal | 32, 3m, $\bar{3}$m | [001] | 0 | 0 | (1) or (3) at $\delta = 0$ | 0 |
| | 3, $\bar{3}$ | [001] | 0 | $\neq 0$ | (5) | see Fig. 6a |
| Hexagonal | 622, 6mm, $\bar{6}$m2, 6/mmm | [001] | 0 | 0 | (1), (3) at $\delta = 0$ | 0 |
| | 6, $\bar{6}$, 6/m | [001] | 0 | $\neq 0$ | (5) | see Fig. 6a |
| Tetragonal | 422, 4mm, 42m, 4/mmm | [001] | $\neq 0$ | 0 | (6) | see Fig. 6b |
| | 4, $\bar{4}$, 4/m | [001] | $\neq 0$ | $\neq 0$ | (4) | see Fig. 6d |
| Cubic | 23, m3, 432, m3m, 43m | [001] | $\neq 0$ | 0 | (6) | see Fig. 6b |
| | | [101] | $\neq 0$ | 0 | (9) | see Fig. 6c |
| | | [*nml*] | $\neq 0$ | 0 | (8) | |

Note: $n, m, l = 0, 1$.

$$\frac{dE_x}{dz} = \frac{3i\pi k_0}{2n_o}\{\chi_{xxxx}[|E_x|^2E_x + {}^1/_3(2|E_y|^2E_x + E_y^2E_x^*)] + \chi_{xxxy}(E_x^2E_y^* + 2|E_x|^2E_y - |E_y|^2E_y)\},$$
$$\frac{dE_y}{dz} = \frac{3i\pi k_0}{2n_o}\{\chi_{xxxx}[|E_y|^2E_y + {}^1/_3(2|E_x|^2E_y + E_x^2E_y^*)] - \chi_{xxxy}(E_y^2E_x^* + 2|E_y|^2E_x - |E_x|^2E_x)\}, \quad (5)$$

$$\frac{dE_x}{dz} = \frac{3i\pi k_0}{2n_o}[\chi_{xxxx}|E_x|^2E_x + \chi_{xxyy}(2|E_y|^2E_x + E_y^2E_x^*)],$$
$$\frac{dE_y}{dz} = \frac{3i\pi k_0}{2n_o}[\chi_{xxxx}|E_y|^2E_y + \chi_{xxyy}(2|E_x|^2E_y + E_x^2E_y^*)], \quad (6)$$

where $n_o$ is the refractive index for the ordinary wave. Due to Kleinman symmetry [22] we used equalities for nonzero components of the tensor $\chi^{(3)}$: $\chi_{xxyy} = \chi_{xyxy} = \chi_{xyyx}$ and $\chi_{xxxy} = \chi_{xxyx} = \chi_{xyxx} = -\chi_{xyyy}$. Generally the XPW efficiency depends on the value of the $B$-integral, the angle $\varphi$ and two anisotropy parameters:

$$\sigma_1 = 1 - 3\chi_{xxyy}/\chi_{xxxx}, \quad \sigma_2 = \chi_{xxxy}/\chi_{xxxx}.$$

Since in practice the angle $\varphi$ may be selected arbitrary, we will assume it to be optimal, i.e., an angle at which the conversion efficiency $\eta$ takes the maximum value $\eta_{max}$.

If $\sigma_2 = \sigma_1 = 0$, i.e., anisotropy of nonlinearity is absent, the system of equations (4), (5) and (6) transforms into system (1). Crystals with the symmetry groups 622, 6mm, $\bar{6}$m2, 6/mmm, 32, 3m, $\bar{3}$m, for which $\sigma_1 = \sigma_2 = 0$ (Table 1), have no anisotropy of nonlinearity (if the optical axis is parallel to $z$ axis) and cannot be used for XPW, i.e., $\eta_{max} = 0$. This is consistent with the results presented in Section 2, because for the linear polarisation the polarisation-ellipse rotation is absent. At the same time, these crystals at low parallelism of the optical axis and the $z$ axis can be used in the scheme described in the previous section (Fig. 3).

If $\sigma_1 = 0$ and $\sigma_2 \neq 0$, which corresponds to crystals with the symmetry groups 3, $\bar{3}$, 6, $\bar{6}$, 6/m, system (4) reduces to (5). The value of $\eta_{max}$ depends only on two parameters: $\sigma_2$ and $B$. The corresponding dependence is shown in Fig. 6a.

If $\sigma_2 = 0$ and $\sigma_1 \neq 0$, which corresponds to the tetragonal crystals with the symmetry groups 422, 4mm, 42m, 4/mm (Table 1), system (4) is transformed into (6), and the value of $\eta_{max}$ depends only on $\sigma_1$ and $B$. The corresponding dependence is shown in Fig. 6b.

If $\sigma_2 \neq 0$ and $\sigma_1 = 0$ (tetragonal crystals with the symmetry groups 4, $\bar{4}$, 4/m), it is necessary to solve system (4). Figure 6d shows the dependence $\eta_{max}(\sigma_1, \sigma_2)$ at $B = 3$. One can see that it is preferable to use crystals with negative $\sigma_1$, while the sign of $\sigma_2$ is irrelevant.

Cubic crystals do not have birefringence, and so the crystal orientation can be arbitrary, and thus, there appear two free parameters – Euler angles $\alpha$ and $\beta$. In this case (Fig. 5), the coordinate system does not coincide with the crystal axes; therefore, the tensor $\chi^{(3)}$ must be transformed using the matrix $U(\alpha,\beta)$ according to the rule [23]

$$\tilde{\chi}_{ijkl} = \sum_{p,q,m,n=1}^{3} U_{ip}U_{jq}U_{km}U_{ln}\chi_{pqmn}, \quad (7)$$

where $\chi_{pqmn}$ are the tensor components in the coordinate system related to the crystal axes; and $\tilde{\chi}_{ijkl}$ are the tensor components in the laboratory frame. The system related to the crystal axes, when Kleinman symmetry for the tensor $\chi^{(3)}$ is fulfilled, has only two independent and nonzero components – $\chi_{xxxx}$ and $\chi_{xxyy}$, i.e., $\sigma_2 = 0$ and $\sigma_1 \neq 0$. A cubic crystal is described by equations (6), the solution of which is shown in Fig. 6c. However, at arbitrary $\alpha$ and $\beta$ after coordinate transformation (7), the tensor $\chi^{(3)}$ has new independent ($\tilde{\chi}_{yyyy}$) and nonzero ($\tilde{\chi}_{xyxx}$, $\tilde{\chi}_{xyyy}$) components, and the system of differential equations for the components of the electric field vector, $E_x$ and $E_y$, takes the form [24]

$$\frac{dE_x}{dz} = \frac{3i\pi k_0}{2n_o}[\tilde{\chi}_{xxxx}|E_x|^2E_x + \tilde{\chi}_{xxyy}(2|E_y|^2E_x + E_y^2E_x^*) + \tilde{\chi}_{xyxx}(2|E_x|^2E_y + E_x^2E_y^*) + \tilde{\chi}_{xyyy}|E_y|^2E_y],$$
$$\frac{dE_y}{dz} = \frac{3i\pi k_0}{2n_o}[\tilde{\chi}_{yyyy}|E_y|^2E_y + \tilde{\chi}_{xxyy}(2|E_x|^2E_y + E_x^2E_y^*) + \tilde{\chi}_{xyyy}(2|E_y|^2E_x + E_y^2E_x^*) + \tilde{\chi}_{xyxx}|E_x|^2E_x]. \quad (8)$$

In the case of crystals with [101] orientation ($\alpha = \pi/4, \beta = 0$), the system of equations (8) is simplified and takes the form

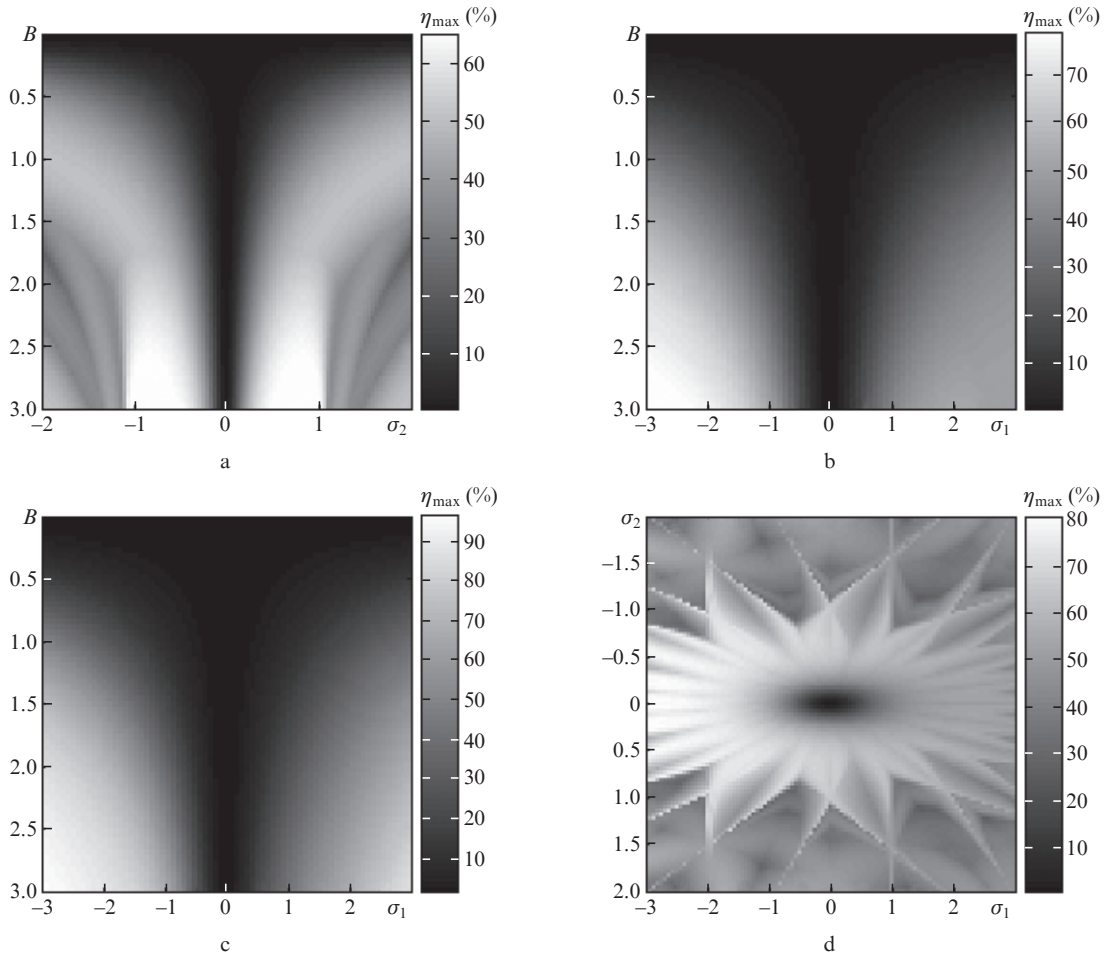


**Figure 6.** Dependences of $\eta_{max}(\sigma_2, B)$ for (a) trigonal or hexagonal crystal with $\sigma_1 = 0$, (b) $\eta_{max}(\sigma_1, B)$ for a tetragonal crystal with $\sigma_2 = 0$ or a cubic crystal with [001] orientation, (c) $\eta_{max}(\sigma_1, B)$ for a cubic crystal with [101] orientation and (d) $\eta_{max}(\sigma_1, \sigma_2)$ at $B = 3$.

$$\frac{dE_x}{dz} = \frac{3i\pi k_0}{2n_o}\chi_{xxxx}\{(1-\sigma_1/2)|E_x|^2E_x + [(1-\sigma_1)/3](2|E_y|^2E_x + E_y^2E_x^*)\},$$
$$\frac{dE_y}{dz} = \frac{3i\pi k_0}{2n_o}\chi_{xxxx}\{|E_y|^2E_y + [(1-\sigma_1)/3](2|E_x|^2E_y + E_x^2E_y^*)\}. \quad (9)$$

Comparison of Figs 6b and 6c shows that the efficiency $\eta_{max}$ in cubic crystals with [101] orientation is slightly greater than in crystals with [001] orientation. The same conclusion was reached in Refs [11, 13]. At the same time it is important to note that this advantage of [101] orientation takes place at the same intensity, i.e., at the same value in the *B*-integral determined by the value of $\chi_{xxxx}$ [see Eqn (2)]. In practice, the value of the *B*-integral is limited by the instability of a plane wave, resulting in small-scale self-focusing [25–27]. Therefore, physically correct is a comparison of different orientations of the cubic crystal with the same instability increment – the value of *h*, which characterises the exponential growth of the amplitude of small-scale harmonic perturbations with a transverse wave vector $\boldsymbol{\kappa}$ against the background of a plane wave [$\propto \cos(\boldsymbol{\kappa} r_\perp)\exp(hz)$] during the development of the instability in a nonlinear medium. This problem was solved for the case of propagation of radiation with linear [28], circular [28] and elliptical [29] polarisations in an isotropic medium. According to the classical paper [28] the maximum instability increment for linear and circular polarisations is equal to the doubled value of the *B*-integral, corresponding to each of the polarisations. The exact determination of the increment for an anisotropic nonlinearity, i.e., for systems of equations (6) and (9), is a separate problem that is outside the scope of this paper. As a rough estimate we can assume that the increment is determined by the arithmetic mean of the diagonal components of the nonlinear susceptibility tensor $\tilde{\chi}_{xxxx}$ and $\tilde{\chi}_{yyyy}$. For [001] orientation this arithmetic mean is equal to $\chi_{xxxx}$, whereas for [101] orientation this mean is equal to $\chi_{xxxx}(1 - \sigma_1/4)$. Thus, an effective *B*-integral for [101] orientation is $1 - \sigma_1/4$ times greater than that of [001] orientation. When the authors of [11, 13] used the parameter $\sigma_1 = -1.2$ for $BaF_2$, the *B*-integral for [101] orientation was 1.3 times greater than that for [001] orientation at the same intensity of radiation. With this in mind, a detailed comparison of Figs 6b and 6c and an analysis of the dependences given in [11, 13] indicate that in the case of physically correct comparison, [001] orientation is better than [101] orientation.

Thus, for a correct comparison of different orientations and a selection of an optimal orientation, one must determine the increment of small-scale instability of a plane wave in a nonlinear anisotropic medium, which for any system of equations [(4)–(6), (8) or (9)] is a separate problem. In this regard,

the question of optimal orientation of a cubic crystal remains open.

Note that even a relatively small increase in efficiency (e.g., from 60% to 75%) may be very significant when using XPW at the output of the last compressor, especially for petawatt radiation, because any loss in this case is particularly important (unlike DCPA). In addition, at the output of high-power laser systems the radiation intensity distribution is typically quasi-uniform and the consequent reduction in efficiency is insignificant. As for the losses caused by the pulse shape, important in many applications is pulse power rather than its energy. Moreover, in a number of applications, pulse compression with a proportional decrease in energy (that is what happens in XPW) can be an additional advantage.

Finally, we discuss which crystals are the most promising for XPW. Measurement of all the components of the nonlinear susceptibility tensor of crystals requires a separate and time-consuming research, which is why data on this issue is scarce in the literature. A review of reference data has shown that the most thoroughly investigated are cubic crystals having two independent components of the tensor $\chi^{(3)}$: $\chi_{xxxx}$ and $\chi_{xxyy}$, whereas the data on uniaxial crystals is scarce (Table 2). In addition, the values of $\sigma_1$, which are presented in various experimental and theoretical studies, can vary by 30%–40% for the same crystal (see data on $SrF_2$ and $BaF_2$), which makes it difficult to choose an optimal crystal.

As shown above, one should choose crystals with a negative value of $\sigma_1$; in this case, the less the $\sigma_1$, the better. According to Table 2 the most promising crystals are CVD-diamond, $SrF_2$, $BaF_2$ and ADP. The first three have a cubic crystal lattice. ADP crystal is uniaxial. Today, $BaF_2$ crystal is most often used in XPW. However, because of incomplete data and differences in the parameter $\sigma_1$, the search for new crystals for highly efficient generation of orthogonally polarised radiation is important. Additionally, uniaxial crystals, practically unused for XPW (except for $YVO_4$ crystal [11]) may also be quite effective.

**Table 2.** Values of the components of the nonlinear susceptibility tensor $\chi^{(3)}$ and the anisotropy parameter $\sigma_1$.

| Crystal | Symmetry group | $\chi_{xxxx}$/ $10^{-22}$ m$^2$ V$^{-2}$ | $\chi_{xxyy}$/ $10^{-22}$ m$^2$ V$^{-2}$ | $\sigma_1 = 1 - 3\chi_{xxyy}/\chi_{xxxx}$ | Ref. |
|---|---|---|---|---|---|
| ADP | 42m | 4.16 | 3.92 | –1.83 | [30] |
| CVD-diamond | m3m | 11 | 10.27 | –1.8 | [31] |
| RbI | m3m | 29.3 | 22.3 | –1.28 | [32] |
| $BaF_2$ | m3m | 1.59 | 1.1 | –1.2 | [33] |
| | | 1.96 | 1.08 | –0.65 | [32] |
| | | 1.45 | 0.96 | –0.99 | [34] |
| $SrF_2$ | m3m | 0.82 | 0.56 | –1.1 | [35] |
| | | 0.98 | 0.59 | –0.8 | [32] |
| | | 1.06 | 0.63 | –0.78 | [34] |
| LiCl | m3m | 7.4 | 5.2 | –1.1 | [32] |
| MgS | m3m | 30.2 | 20 | –0.98 | [32] |
| $CaF_2$ | m3m | 1.1 | 0.55 | –0.5 | [32] |
| | | 0.9 | 0.5 | –0.65 | [34] |
| MgO | m3m | 5.6 | 2.9 | –0.58 | [32] |
| | | 4.1 | 1.98 | –0.45 | [34] |
| LiF | m3m | 0.73 | 0.34 | –0.4 | [32] |
| | | 0.53 | 0.24 | –0.36 | [34] |
| C-diamond | m3m | 6.95 | 2.95 | –0.27 | [35] |
| $YVO_4$ | 4/mmm | 13 | –0.43 | 1.1 | [11] |
| KDP | 42m | 1.73 | 0.24 | 0.58 | [34] |
| | | 3.49 | 0.49 | 0.58 | [36] |
| | | 1.99 | 0.28 | 0.58 | [37] |
| | | 3.3 | 0.56 | 0.5 | [38] |
| $TiO_2$ | 4/mmm | 128.25 | 25.65 | 0.4 | [39] |
| GGG | m3m | 11.95 | 3.22 | 0.19 | [39] |

## 5. Conclusions

In this paper we have considered two methods of enhancing the temporal contrast of high-power radiation, based on the effect of cubic nonlinearity on the polarisation of laser radiation. The first method investigates the change in the polarisation of radiation propagating in a weakly anisotropic medium with an isotropic nonlinearity. We have proposed a new scheme, which consists of two identical NEs with axes rotated through 90° relative to each other. It is shown that the effectiveness of this method is comparable to the efficiency of the method, which uses a nonlinear isotropic medium (at $B > 3$ even exceeds it).

The second method of contrast enhancement is based on the generation of an orthogonally polarised component of radiation in an anisotropic medium with cubic nonlinearity. We have obtained the dependences of the maximum generation efficiency $\eta_{max}$ on the nonlinearity tensor anisotropy parameters $\sigma_1$ and $\sigma_2$, as well as on the value of the $B$-integral for uniaxial and cubic crystals of all types of symmetry. It is shown that for the correct determination of the optimum orientation of a cubic crystal it is necessary for each orientation to determine an effective $B$-integral. To this end it is needed to calculate the increment of the small-scale self-focusing instability in a nonlinear anisotropic medium. This problem is of interest and is the subject of further research.

## References


1. Yanovsky V.P., Perry M.D., Brown C.G., Feit M.D., Rubenchik A. *Proc. Ultrafast Optics Conf.* (Monterey, CA, 1997) paper WD-2.
2. Doumy G., Quere F., Gobert O., Pedrix M., Martin Ph., Audebert P., Gauthier J.C., Geindre J.-P., Wittmann T. *Phys. Rev. E*, **69**, 026402 (2004).
3. Mironov S., Lozhkarev V., Ginzburg V., Khazanov E. *J. Appl. Opt.*, **48**, 2051 (2009).
4. Mironov S.Y., Lozhkarev V.V., Ginzburg V.N., Yakovlev I.V., Luchinin G., Shaykin A.A., Khazanov E.A., Babin A.A., Novikov E., Fadeev S., Sergeev A.M., Mourou G.A. *IEEE J. Sel. Top. Quantum Electron.*, **18** (1), 7 (2012).
5. Kalashnikov M.P., Risse E., Schönnagel H., Sandner W. *Opt. Lett.*, **30** (8), 923 (2005).
6. Renault A., Auge-Rochereau F., Planchon T., d'Oliveira P., Auguste T., Chériaux G., Chambaret J.-P. *Opt. Commun.*, **248**, 535 (2005).
7. Itatani J., Faure J., Nantel M., Mourou G., Watanabe S. *Opt. Commun.*, **148**, 70 (1998).
8. Yanovsky V., Saleh N., Milathianaki D., Felix C., Flippo K., Nees J., Maksimchuk A., Umstadter D., Mourou G., Squicr J. *Proc. Conf. on Lasers and Electro-Optics (CLEO'2000)* (Nice, 2000) Vol. 39, paper CWK2.
9. Homoelle D., Gaeta A.L., Yanovsky V., Mourou G. *Opt. Lett.*, **27** (18), 1646 (2002).
10. Jullien A., Auge-Rochereau F., Cheriaux G., Chambaret J.-P., d'Oliveira P., Augusta T., Falcoz F. *Opt. Lett.*, **29**, 2184 (2004).
11. Minkovski N., Petrov G.I., Saltiel S.M., Albert O., Etchepare J. *J. Opt. Soc. Am. B*, **21**, 1659 (2004).
12. Jullien A., Albert O., Burgy F., Hamoniaux G., Rousseau J.-P., Chambaret J.-P., Auge-Rocherau F., Cheriaux G., Etchepare J., Minkovski N., Saltiel S. *Opt. Lett.*, **30**, 920 (2005).
13. Ramirez L.P., Papadopoulos D., Hanna M., Pellegrina A., Friebel F., Georges P., Druon F. *J. Opt. Soc. Am. B*, **30** (10), 2607 (2013).
14. Liu J., Okamura K., Kida Y., Kobayashi T. *Opt. Express*, **18** (21), 22245 (2010).

15. Vlasov S.N., Kryzhanovskii V.I., Yashin V.E. *Kvantovaya Elektron*., **9** (1), 14 (1982) [*Quantum Electron*., **12** (1), 7 (1982)].
16. Vlasov D.V., Korobkin V.V., Serov R.V. *Kvantovaya Elektron*., **6** (7), 1542 (1979) [*Quantum Electron*., **9** (7), 904 (1979)].
17. Fibich G., Ilan B. *Phys. Rev. E*, **67** (3), 036622 (2003).
18. Kuzmina M.S., Martyanov M.A., Poteomkin A.K., Khazanov E.A., Shaykin A.A. *Opt. Express*, **19** (22), 21977 (2011).
19. Oda M., Nemat-Nasser S., Konishi J. *Soils and Foundations*, **25** (3), 85 (1985).
20. Deyra L., Balembois F., Guilbaud A., Villeval P., Georges P. *Opt. Express*, **22** (19), 23315 (2014).
21. Kochetkova M.S., Martyanov M.A., Poteomkin A.K., Khazanov E.A. *Opt. Express*, **18** (12), 12839 (2010).
22. Sutherland R. *Handbook of Nonlinear Optics* (New York: Basel, 2003).
23. Korn G., Korn T. *Mathematical Handbook for Scientists and Engineers* (New York: McGraw-Hill, 1968; Moscow: Nauka, 1984).
24. Kourtev S., Minkovski N., Canova L., Jullien A., Albert O., Saltiel S.M. *J. Opt. Soc. Am. B*, **26** (7), 1269 (2009).
25. Bespalov V.I., Talanov V.I. *Pis'ma Zh. Eksp. Teor. Fiz.*, **3**, 471 (1966).
26. Brown D.C. *High-Peak-Power Lasers* (Berlin–Heidelberg–New York: Springer, 1981).
27. Mak A.A., Soms L.N., Fromzel V.A., Yashin V.E. *Lazery na neodimovom stekle* (Neodymium Glass Lasers) (Moscow: Nauka, 1990).
28. Rozanov N.N., Smirnov V.A. *Kvantovaya Elektron.*, **7** (2), 410 (1980) [*Quantum Electron*., **10** (2), 232 (1980)].
29. Kuz'mina M.S., Khazanov E.A. *Kvantovaya Elektron*., **43** (1), 21 (2013) [*Quantum Electron*., **43** (1), 21 (2013)].
30. Wang C.C., Baardsen E.L. *Appl. Phys. Lett*., **70**, 396 (1969).
31. http://www.cvd-diamond.com/.
32. Ching W.Y., Gan F., Huang Ming-Zhu. *Phys. Rev. B*, **52** (3), 1596 (1995).
33. DeSalvo R., Sheik-Behae M., Said A.A., Hagan D.J., Van Stryland E.W. *Opt. Lett*., **18** (3), 194 (1993).
34. Adair R., Chase L.L., Payne S.A. *Phys. Rev. B*, **39**, 3337 (1989).
35. Levenson M.D., Bloembergen N. *Phys. Rev. B*, **10**, 4447 (1974).
36. Kulagin I.A., Ganeev R.A., Tugushev R.I., Ryasnyansky A.I., Usmanov T. *J. Opt. Soc. Am. B*, **23** (1), 75 (2006).
37. Prokhorov A.M. (Ed.) *Spravochnik po lazeram* (Laser Handbook) (Moscow: Sov. radio, 1978) Vol. 2.
38. Eichler H.J., Fery H., Knof J., Eichler J. *Z. Physik B*, **28**, 297 (1977).
39. Petrocelli G., Pichini E., Scudieri F., Martellucci S. *J. Opt. Soc. Am. B*, **10**, 918 (1993).